Overview of Underwater Transmission Characteristics of Oceanic LiDAR

Guoqing Zhou, *Senior Member, IEEE*, Chenyang Li, Dianjun Zhang, Dequan Liu, Xiang Zhou, and Jie Zhan

***Abstract*—Oceanic LiDAR (hereafter referred to as O-LiDAR) is an important remote sensing device for measuring the near-coastal water depth and for studying the optical properties of water bodies. With the commercialization of LiDAR, the theoretical research on the underwater transmission characteristics of LiDAR has been intensified worldwide. Primary research interests include the simulation and modeling of LiDAR underwater echo signals and the inversion of optical parameters using LiDAR water echo signals. This article provides an overview of the principle of LiDAR echo signal formation, and comprehensively summarizes the LiDAR echo signal simulation modeling methods and the corresponding factors that affect modeling accuracy by focusing on the characteristics of different methods. We found that the current simulation methods of LiDAR underwater transmission echo signals primarily include an analytical method based on the radiation transfer equation and a statistical method based on the Monte Carlo (MC) model. The radiation transport equation needs to be appropriately simplified using the analytical method, usually using the quasi-single-small-angle approximation principle. The analytical method has high calculation efficiency but its accuracy is dependent to the quasi-single small-angle approximation. The statistical method can analyze the influence of various factors on echo signals by controlling the variables, but it has poor calculation efficiency. Finally, the semianalytical MC model was used to quantitatively analyze the three main factors (LiDAR system parameters, water body optical parameters, and environmental parameters) affecting underwater LiDAR transmission characteristics, and summarizes the mechanism and results of different factors.**

***Index Terms*—Oceanic LiDAR (O-LiDAR), echo signal simulation method, analytical method, Monte Carlo (MC).**

Manuscript received June 8, 2021; revised July 19, 2021; accepted July 22, 2021. Date of publication July 27, 2021; date of current version August 30, 2021. This work was supported in part by the National Natural Science of China under Grants 41961065 and 41431179, in part by the Guangxi Innovative Development Grand Program under Grants Guike AD19254002, GuikeAA18118038, and GuikeAA18242048, in part by the Guangxi Natural Science Foundation for Innovation Research Team under Grant 2019GXNSFGA245001, in part by the Guilin Research and Development Plan Program under Grant 201902102, in part by the National Key Research and Development Program of China under Grant 2016YFB0502501, in part by the BaGuiScholars Program of Guangxi, and in part by the Open Fund of Guangxi Key Laboratory of spatial Information and Geomatics under Grants 19-050-11-11 and 19-185-10-19. *(Corresponding author: Chenyang Li.)*

Guoqing Zhou and Xiang Zhou are with the School of Microelectronics, Tianjin University, Tianjin 300072, China, and also with the Guang Xi Key Laboratory for Spatial Information and Geomatics, Guilin University of Technology, Guilin 541004, China (e-mail: gzhou@glut.edu.cn; zqx0711@tju.edu.cn).

Chenyang Li, Dianjun Zhang, and Jie Zhan are with the School of Marine Science and Technology, Tianjin University, Tianjin 300072, China (e-mail: 1019227006@tju.edu.cn; zhangdj@tju.edu.cn; 2019227025@tju.edu.cn).

Dequan Liu is with the School of Microelectronics, Tianjin University, Tianjin 300072, China (e-mail: 1017232001@tju.edu.cn).

Digital Object Identifier 10.1109/JSTARS.2021.3100395

I. Introduction

SINCE the establishment of the first system in the 1960s, research on laser bathymetry technology has been extensively funded by governments and other institutions worldwide (e.g., the USA, Canada, Australia, Sweden, Austria, and China). After the initial, developmental, and commercial stages in the 1960s–1980s, 1980s–1990s, and 1990s–2000s, respectively, the current mainstream international airborne LiDAR bathymetric system entered the stage of full commercialization [1]. O-LiDAR technology is an important component of optical remote sensing technology that compensates for the shortcomings of passive aquatic remote sensing and conveniently obtains ocean hydrographic, bathymetric, and seafloor topographic information because of its rich piggyback platform, independence on day and night environments, ability to obtain information on the vertical distribution of seawater optical parameters, and measurement accuracy meeting IHO Class I standards. O-LiDAR is widely used in military and civil fields for underwater communication [2], underwater topography mapping [3], [4], hydrographic parameter telemetry [5], and marine environmental pollution monitoring. LiDAR technology has achieved substantial advancement in the field of high-resolution optical remote sensing [6]–[8]. Further development of the technology in the field of ocean exploration would improve the marine optical remote sensing three-dimensional observation network and help solve the increasingly prominent development problems of marine environmental protection, marine resource development, and maritime right maintenance [9]–[12], [84].

When a laser is transmitted in a water body, the energy is markedly attenuated by the absorption and scattering of water molecules and suspended particles, thus shifting the transmitted beam and expanding the spot. The study of laser transmission characteristics in water bodies and quantitative analysis of the beam energy attenuation law provide fundamental theoretical support for the accurate establishment of LiDAR bathymetric equations, the establishment of signal attenuation models for each transmission process, the simulation of LiDAR echo signals, and the study of echo signal processing methods that are key to the development of future-oriented O-LiDAR systems. Current international O-LiDAR system research and development teams have conducted in-depth research on the characteristics of underwater laser transmission to achieve high-precision ocean exploration. In this article, we present a detailed overview and comprehensive analysis of the research results of the last 50 years in the field of laser underwater transmission characteristics worldwide. The purposes of this review are to provide an

improved understanding of the laser underwater transmission characteristics of O-LiDAR systems.

II. Review of O-LiDAR Laser Underwater Transmission Characteristics Study

As early as 1957, Hulst and Twersky [13] proposed the theory of small particle scattering, laying the foundation of radiative transfer theory in light scattering-related research. In 1968, Hickman and Hogg [14] at Syracuse University developed the first laser seawater depth measurement system, conducted the first feasibility study of laser underwater bathymetry measurement technology, and provided a theoretical basis for using laser sounding technology. Since then, the U.S. Navy has focused on the characteristics of laser underwater transmission and the prospect of underwater laser applications. Teams used research by Duntley [15] to study underwater laser transmission, ushering in a second decade of research programs (from 1958 to 1966) based on the theoretical basis of the first decade of research. The initial phase (1958–1960) primarily included analysis of the radiation transmission pattern of underwater conventional light source illumination. Because of the unavailability of underwater lasers, researchers used incandescent underwater projectors from 1961 to 1964 to analyze the underwater transmission patterns of collimated beams produced by projectors. From 1964 to 1966, Duntley [15] conducted underwater laser experiments using an RCA laser in Lake Winnipesaukee on Diamond Island to reduce the cost and difficulties of sea-based experiments, to understand the principles of light transmission in water, and to refine experimental techniques. The transmission experiments during this period showed that the power of the scattered radiation from the collimated beam depended on the volume attenuation coefficient ratio. In 1965, Preisendorfer *et al.* [16] outlined how Maxwell's equations could be converted to obtain the radiation transport equation (RTE) applicable to the principle of radiation interaction inside a medium. This article that solved RTE using the invariant embedding theory and other analytical methods, represents a framework for elucidating the internal structure of radiative transfer theory. In 1966, Sorenson *et al.* [17] obtained an empirical formula for point diffusion function but did not provide a method for establishing the formula. The part of the formula consists of 12 parameters, obtained by fitting, with no obvious physical significance. In the late 1960s, Plass, Kattanwar, Collins, and others [18]–[20] invoked the standard Monte Carlo (MC) method in the study of light scattering; the method gradually became one of the most common in light scattering studies. In 1968, Plass and Kattawar [18] first introduced the MC method for radiative transfer modeling to simulate solar transport and backscattering in the atmosphere and seawater. Subsequently, Bruscaglioni, Starkov, Winker, and Poole [21]–[24] developed effective MC models.

In the 1970s, Arnush [29] obtained a formula for beam diffusion function for artificial seawater by studying the optical radiation transmission properties of lasers under Mie scattering conditions using 17 fitted parameters interpolated in the 10-year research results of laser underwater transmission. Empirical equations of off-axis irradiance were established to obtain approximate analytical values of the optical field for laser transmission in seawater to facilitate the study of the transmission performance of underwater laser systems in other types of water and at other wavelengths. In 1972, Pelzold [26] obtained the scattering phase function in water by external field empirical measurements and found that the scattered light energy of laser transmission in water is primarily concentrated in the forward direction with a symmetric trend; additionally, the probability of backward scattering near 180° was basically zero. In the same year, Yura [27] studied the principle of small-angle scattering from seawater. In 1972, D. Arnush [29] used the forward scattering properties of scattering media (e.g., the atmosphere and seawater) and obtained the forward scattering characteristic medium radiation transmission equation by simplifying the classical radiation transmission equation to establish a mathematical model of multiple forward scattering with small-angle approximation. In 1977, Acquista and Anderson [42] derived the RTE from the laws of quantum electrodynamics. In 1978, Stotts [30] introduced a formula for pulse time expansion in multiple scattering media with forward scattering properties. In the same year, Lutomirski [31] used radiative transfer and Green's function to determine the relationship between the depth and spatial distribution of radiation.

In 1981, Fante [32] rigorously derived the RTE equations using Maxwell's equations. 1981, Poole *et al.* [33] improved the conventional MC to semianalytic MC simulation by introducing a stochastic process and statistical estimation method to calculate the probability of the photon returning directly to the receiver after each occurrence of scattering, reducing the statistical uncertainty of the data. They established the O-LiDAR semi-analytic MC simulation model SALMON, which is much more computationally efficient than the conventional MC method. In 1982, SALMON was experimentally validated in the laboratory [34]; the performance of fluorescence LiDAR based on Raman correction was evaluated using this model. In 1982, Gordon [35] used the SALMON model to analyze the effect of multiple scattering on the effective attenuation coefficient and the backscatter coefficient of airborne O-LiDAR. The relationship among the effective attenuation coefficient of LiDAR, the parameters of the LiDAR system, and the parameters of the optical properties of the water body were analyzed. Further, researchers proposed that the LiDAR attenuation coefficient is closely related to the field of view, the size of which corresponds to the variation of the effective attenuation coefficient between the beam attenuation coefficient and the diffuse attenuation coefficient—which is still widely used in O-LiDAR signal inversion. In 1982, Baker and Smith [36] developed a bio-optical model that was used to establish the relationship between the optical properties of near-surface seawater and its biological content, to provide a quantitative description of the intrinsic and apparent optical properties, and to establish the relationship between the apparent and intrinsic optical properties and the inversion algorithm. In 1986, Stamnes [37] used the Boltzmann equation to derive the RTE equation from the concept of photons. In 1987, Mobley [38] derived the intuitive and mathematically simple RTE equation,

which has physical significance. In 1989, Gordon [39] used the Lambert-Beer law as a theoretical model for simulating underwater optical transmission.

In 1995, Wang *et al*. [40] developed the MC model MCML for the radiative transfer of light in a layered medium using C. The model completely simulated the process of light beam incidence on a body of water until the photon leaves the water or is absorbed, recording the reflection and transmission process of photons in water. In 1997, Katsev *et al.* [41]. derived the LiDAR equation in Fourier space, which has a very intuitive physical meaning. In 1999, Walker and McLean [43] used small-angle approximation to derive a LiDAR equation applicable to homogeneous water bodies. In 1998, Krekov *et al*. [44] used the MC method to study the O-LiDAR signal characteristics for the detection of stratified water bodies.

In 2004, Gimond [45] wrote the AOMC aquatic optical MC model using the Fortran language. The AOMC model simulates the propagation of light in an optically shallow, vertically inhomogeneous aquatic medium. In 2003 and 2008, Kopilevich *et al.* [46], [93] derived the mathematical model of returned O-LiDAR signals developed by Dolin and Levin *et al.* The model was proposed based on an analytical solution of the RTE in seawater using the small-angle scattering approximation. In 2012, Abdallah *et al.* [47] used the underwater radiative transfer model to fully consider the entire process of laser bathymetric transmission. Their expressions include instantaneous echo power at the water surface, instantaneous echo power in the water body, instantaneous echo power at the bottom of the water, background noise power, and internal noise power inside the instrument to establish the airborne laser bathymetric LiDAR equations for the Wa-LiD model. In 2016, Kim *et al*. [50] used Green's function, optical reciprocity theorem, and small-angle approximation theory to derive the general LiDAR equation. The equation is solved by the Fourier transform method to obtain the radiation distribution of the RTE, and the derived LiDAR equation is used for CZMIL laser echo signal modeling. In 2020, Liu *et al*. [49] combined an MC simulation with LiDAR outfield experiments to demonstrate the MC LiDAR calibration potential and introduce the MC method into the O-LiDAR experimental validation study. In 2021, Mayesffer *et al*. [48] used the MC method to simulate photon transmission through a turbid medium by Mie scattering.

Summarizing more than 50 years of literature related to laser underwater transmission characteristics to quantitatively study the energy attenuation law and light field distribution characteristics of laser transmission in water reveals an emphasis on the following research aspects.

1) Principle of underwater transmission echo signal formation.
2) Simulation model building study of LiDAR underwater echo signals.
3) Quantitative analysis of the effects of different factors on echo signals.

We later present a more detailed review and analysis of the three research directions.

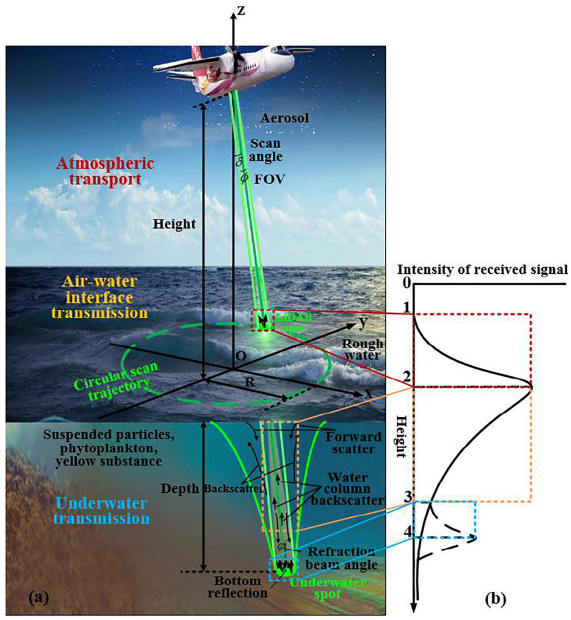

Fig. 1. Detection schematic diagram of O-LiDAR, (a) Laser transmission. (b) Echo signal generation.

III. Basic Principle of LiDAR Echo Signal Formation

When O-LiDAR detects seawater, the emitter emits a collimated blue-green laser pulse with high energy, narrow pulse width and high beam quality that passes through the atmosphere and the air-water interface through the downward channel and is transmitted underwater to the target. During this process, the laser is reflected, transmitted, scattered and absorbed by the water surface and water body, and then is reflected by the bottom target. The reflected laser pulse signal reaches the laser receiver through the uplink channel in the opposite direction, and the receiver stores the echo signal. Fig. 1(a) shows a schematic diagram of the transmission. The transmission of the laser pulse through the entire link produces a series of linear and nonlinear effects and leads to the formation of a complex functional relationship between the transmitted pulse energy, the received energy, and the laser transmission time. Fig. 1(b) shows the laser LiDAR echo signal; the abscissa is the detection depth, the ordinate is the echo signal. The echo signals at 1-2, 2-3, 3-4 of Fig. 1(b) come from the reflection or backscattering of signals from water surface, water body, bottom and phytoplankton respectively. In Sections II and III, the laser is attenuated by the absorption and scattering of the water body in seawater. The focus of this overview and analysis is on sections II and III of Fig. 1(b). Analyzing the phase, frequency, amplitude, and polarization of the echo signal after laser transmission inverts the optical characteristics of the detected target to obtain the surface state, composition, material concentration, and spatial distribution characteristics of the object and the profile distribution of different ocean parameters.

When the laser is transmitted in water, the echo power of each part received by the receiver can be regarded as the convolution

of the echo signal of each part of the LiDAR and the system response w. When considering only the outgoing laser waveform, the system response changes with time approximately as a Gaussian distribution. The echo power $P_c(t)$ of the water body can be expressed as [47]

$$\begin{cases} P_c(t) = \int w(t_c)P(z)dz \\ w(t_c) = \frac{2}{T_0}\sqrt{\frac{\ln 2}{\pi}}\exp\left[-4\ln 2\frac{(t-t_c)^2}{T_0^2}\right] \\ t_c = \frac{2H}{v} + \frac{2nz}{v} \end{cases} \quad (1)$$

where t_c is the two-way time delay between the detector and the water body, H is the working height of the LiDAR, T_0 is the full width at half height of Gaussian distribution, and $P(z)$ is the water body LiDAR equation.

When O-LiDAR laser propagates underwater, the general LiDAR equation $P(z)$ of backward elastic scattering of the water body can be expressed as [54], [56]

$$P(z) = \frac{P_0 A_r \eta O(z) T (1-l_s)^2}{(nH+z)^2}\frac{v\Delta t}{2n}(\beta_z^p(z) + \beta_z^w(z))\exp\left[-2\int_0^z (a^p(z') + a^w(z'))dz'\right] \quad (2)$$

where P_0 is the average power of the initially emitted laser pulse, A_r is the receiving aperture area, η is the photoelectric conversion efficiency of the detector (determined by the type of material of the photodetector), $O(z) = \frac{A_t}{A_l}$ is the overlap coefficient of the detection targets (between 0 and 1, which mainly affects atmospheric signals); A_t is the illuminated area of the target, A_l is the spot area, n is the refractive index of seawater; H is the height of the aircraft from the sea surface, z is the water depth, l_s is the Fresnel Reflection coefficient (the value is usually 0.02 for a perpendicularly incident laser on the sea surface); *T* is the transmittance of the receiving aperture, *v* is the propagation speed of light in vacuum, $\beta_\pi(z) = \beta_\pi^p(z) + \beta_\pi^w(z)$ is the phase function of the 180° scattering angle, $\alpha(z') = \alpha^p(z') + \alpha^w(z')$ is the effective attenuation coefficient of LiDAR, and the superscripts *p* and *w* are expressed as suspended solids and pure water in the water body, respectively.

IV. LiDAR Echo Signal Simulation Method

LiDAR experts and scholars worldwide use two principal research methods.

1) Field experiment method [15].
2) Theoretical simulation method [57].

The selection of the field experiment method was primarily concentrated in the 1960s and 1970s. A theoretical simulation method had not yet been developed. Therefore, the energy value of the laser at different water depths was measured by instruments through a field experiment method; the underwater beam transmission characteristic curve with special optical characteristics was obtained by fitting. The advantage of the field experiment method is that the measurement results are intuitive and conform to the actual physical process of beam transmission. The principal disadvantage is the high cost of field experiments. Accurately controlling the single variable condition of a water environment not conducive to quantitative analysis of the influencing factors of energy attenuation of lasers transmitted in water is difficult. In the late 1970s, the establishment and solution methods of the numerical model of radiation theory became increasingly perfect. In the 1980s, the theory of echo signal simulation matured with the establishment of the semianalytical MC method.

According to the differences established by the models, the theoretical simulation methods include the following.

1) Maxwell equation theoretical model based on photon wave characteristics [16], [51].
2) Stochastic model [28], [58].
3) Theoretical model of radiative transfer equation based on photon particle characteristics [52], [53].
4) Diffusion approximation theory [62].
5) MC simulation model based on statistical methods [33], [59].

Since the early 1960s, the RTE and MC models have been the mainstream LiDAR echo signal simulation models. The two models adapt to different environmental conditions, have corresponding advantages and disadvantages, cannot replace each other, and have been simultaneously developed since their establishment.

A. Radiative Transfer Equation Model

The RTE was established based on the particle characteristics of light and satisfies the law of conservation of energy while ignoring the wave effect of light. The RTE is primarily suitable for describing the propagation of light in a medium where the distance between particles is much larger than the wavelength of the light source. The radiative transfer theory efficiently simulates multiple LiDAR scattering echo signals. The RTE consists of a variety of independent variables, and the formula is a complex calculus equation. A direct solution needs to assume a variety of ideal conditions, such as homologous optical characteristics of the water body, a horizontal sea level, the sun as a point source in a dark sky, lack of an internal source, and single scattering of photons. The approximate solution of the equation is obtained by simplifying the transmission equation. Therefore, in recent years, research on radiative transfer equation models has primarily focused on the solution method of the radiative transfer equation. Commonly used methods to solve the radiative transfer equation include the following.

1) Invariant imbedding method [60], [61].
2) Discrete coordinate method [63], [67].
3) Spherical harmonic expansion [68].

Their respective characteristics primarily include the following.

1) *Invariant imbedding method:* In 1988, Preisendorfer and Mobley [60], [61] established the invariant imbedding method (II method), which was transformed into the Riccati differential equation on radiance L by Fourier analysis and invariant imbedding theory to obtain the numerical solution.

Algorithm features [57] the following.

a) Highly mathematical analysis.

b) Difficult to program.
c) Only solves a 1-D problem (1-D refers to depth information).
d) Including multiple scattering.
e) No statistical error in the radiation result.
f) Fast running speed (running time increases linearly with depth).
g) Most extensively applied method for solving the radiation equation of water bodies.

Advantages include the high computational efficiency and the ease of obtaining accurate radiation distribution for large depths because the calculation time is a linear function of depth. The calculation time depends only slightly on the scattering attenuation ratio, surface boundary conditions, and water stratification.

Application: In 1995, Mobley [69] used the invariant imbedding method to compile and establish the Hydrolight radiative transfer model in Fortran to solve the radiative transfer equation to obtain the radiance changes with water depth, zenith angle, azimuth angle, wavelength, and other distributions; additionally, they obtained the radiation distribution and spectral intensity independent of time inside and outside the water body in any plane.

2) *Discrete Ordinate Method:* In 1994, Jin and Stamnes [63] used the discrete ordinate method to solve the problem of radiation transmission between systems with different refractive indices. The method is often used to analyze the steady-state radiative transfer equation of a laser in an atmosphere-ocean coupling transmission system and transforms the integrodifferential equation into a coupled ordinary differential equation solved by the discrete ordinate method.

Characteristics of the discrete ordinate method [57] are as follows.

a) The calculation speed is directly proportional to the number of horizontal layers used to analyze the optical characteristics of oceans.
b) Accurate irradiance can be obtained with only a small data stream, thus improving the code execution efficiency.
c) Radiation and irradiance can be returned at any optical depth independent of the calculation level.
d) The method is essentially a matrix eigenvalue-eigenvector solution from which the corresponding solution is automatically obtained.
e) The inelastic scattering effect is calculated to address phenomena, such as Raman scattering.
f) The method includes a wind-blown surface to simulate the basic characteristics of ocean surface roughness.
g) The method cannot deal with the high peak scattering phase function well and is unsuitable for water with great IOPs variation with depth.

Application: In 1996, Anderson *et al.* [70] combined the principle of solving the radiative transfer equation using the discrete coordinate method and compiled the MODTRAN model in Fortran language to analyze atmospheric radiative transfer. The path transmittance, atmospheric emissivity, single (multiple) scattering solar/lunar emissivity, medium spectral resolution, and atmospheric transmittance of absorbing substances can be calculated.

3) *Spherical Harmonic Expansion Method:* In 1998, Evans [71] used the spherical harmonic expansion method to solve the radiative transfer equation. The emissivity and phase functions can be expanded using the spherical harmonic function as the basis function. First- and third-order spherical harmonic expansions are widely used to approximate the radiation equation. The finite element [72] and discrete solid angle [63] methods are often used to complete the calculation for numerical simulation in the solution process.

Because the radiative transfer equation needs to be approximately simplified in the solution, the principal solution methods developed to date include the following.

1) *Single scattering approximation:* the mainstream approximation method and suitable for optical thin media, such as in the medical field [52], [73].
2) *Asymptotic approximation:* suitable for solving the light field in a thick optical medium [95].
3) *Diffusion approximation:* usually obtained using the first-order spherical harmonic expansion approximation. Suitable for all identical media [62].
4) Phenomenological equation approximation [25].
5) *Small angle approximation:* Suitable for medium with peak forward scattering and medium optical thickness, such as offshore waters [41], [75].

In marine applications (especially LiDAR near-coast bathymetry), the principle of small-angle approximation is preferred. According to this principle, the complex multiple scattering process is simplified into one backward single scattering and two forward multiple scatterings. Researchers primarily use the LiDAR equation obtained by Katsev *et al.* [41] by Fourier transform when using the precision LiDAR equation derived from radiation transmission to simulate echo signals. The equation is expressed as follows:

$$P(z) = W_0 \frac{b(z)}{4\pi} \frac{V}{2} \int d\mathbf{r} \int d\mathbf{\Omega}' \int \mathbf{\Omega}'' \beta_\pi(z; |\mathbf{\Omega}' - \mathbf{\Omega}''|) \times I_{\mathrm{src}}(z, \mathbf{r}, \mathbf{\Omega}') I_{\mathrm{src}}^{\mathrm{rec}}(z, \mathbf{r}, \mathbf{\Omega}'') \quad (3)$$

where W_0 is the laser pulse energy, z is the detection depth; V is the velocity of laser propagation in water; vector $\mathbf{r}$ represents the projection of the scattering surface; and vectors $\mathbf{\Omega}'$ and $\mathbf{\Omega}''$ represent the projection of the laser transmission direction on the scattering surface; b is the scattering coefficient, and β_π is the 180° backscattering phase function; I_{src} and $I_{\mathrm{src}}^{\mathrm{rec}}$ are the real and virtual powers of the light source and the receiver at the scattering position, respectively, which describe the change laser radiation from the exit position to the scattering position and is approximately a two-stage forward scattering process; β_{back} describes a single backscattering at a single scattering position. According to the principle of small-angle approximation, the probability of backscattering is very small; thus, the forward scattering coefficient can be approximated as the total scattering coefficient.

The advantages and disadvantages of using radiative transfer equation model to study laser underwater transmission characteristics are summarized as follows.

Advantages: The analytical model quickly and efficiently simulates multiple LiDAR scattering signals. The LiDAR equation was derived using the analytical model, which greatly reduces the complexity and calculation cost of multiple scattering and greatly improves the calculation efficiency [50].

Disadvantages: When using this analytical method to solve the radiative transfer equation, some approximations are made to simplify the complex computation processes; thus, the obtained analytical solution is usually an approximate solution of the radiative transfer equation, reducing the accuracy of the analytical model.

B. MC Simulation Model

The MC model is a statistical simulation method based on an MC algorithm model. The process of laser beam absorption and scattering by water particles during radiation transmission can be expressed intuitively. The standard MC simulation assumes that the propagation path of the laser in water is composed of many completely random photon tracks. Quantitative analysis of the basic scattering and absorption characteristics of the medium defines the scattering and absorption probabilities, the probability of scattering in each direction, and the probability distribution of the random walk step size; thus, the probability distribution function of the length and direction of each trajectory segment can be explained. Furthermore, the integral values of the photons under different parameter settings are used to calculate physical quantities of interest, such as the LiDAR echo signals [18]. The advantage of this method is the greatest overall similarity to the real LiDAR signal transmission process. However, owing to the low backscattering probability in the transmission process, the fixed receiving field angle of the receiver, and the limited receiving aperture and area of the receiver, only a few simulated photons meet the receiving conditions. A large statistical error occurs if the number of simulated photons is insufficient. In 1981, Poole *et al*. [33] improved the standard MC into a semianalytical MC simulation by introducing a stochastic process and statistical estimation method to calculate the probability of photons returning directly to the receiver after each scattering, thus reducing the uncertainty of the data statistics. The semianalytical MC simulation model SALMON (established by Poole *et al*.) greatly improves the computational efficiency compared with the standard MC method.

The estimated or expected value of the semianalytical probability is expressed as [12], [49], [74], [76], [92], [94]

$$\begin{cases} p(z) = \frac{\beta(\theta',z)}{4\pi} \frac{A_r}{\left(\frac{H+z_i}{\cos\phi}\right)^2} \exp(-\sum_{i=1}^{i} c(i)d')T_s w(i) \\ i = \mathrm{round}(\frac{z}{\Delta z}) \\ \cos\theta' = u_x u'_{1x} + u_y u'_{1y} + u_z u'_{1z} \\ u'_{1x} = -\frac{x}{\sqrt{x^2+y^2+(nH+z)^2}} \\ u'_{1y} = -\frac{y}{\sqrt{x^2+y^2+(nH+z)^2}} \\ u'_{1z} = -\sqrt{1-u_x^2-u_y^2} \end{cases} \tag{4}$$

where $p(z)$ is the received probability signal at depth z; i is the layer index; Δz is the thickness of each divided layer; $\beta(\theta', z)$ is assumed to be a constant scattering phase function at a small solid angle $\Delta\Omega$ at a water depth z; H is the LiDAR working height; z_i is the photon depth in the i-=th layer; A_r is the detection aperture area; $\exp(-cd'_i)$ is the probability of photons scattered to the detector by angle θ' and no longer interacting with the medium; $d'_i = z_i/\sqrt{1-(\sin\varphi/n)^2}$ is the distance of the current scattering point to the sea surface along $\vec{\varepsilon'}$; φ is the incident angle of the laser from the atmosphere to water; n is the refractive index of seawater; T_s is the Fresnel transmittance of the air-water interface, and $w(i)$ is the weight of presently scattered photons. For very small φ values, d'_i is approximately the depth of each layer of water, and the transmission distance is approximately $H + z_i$. Every time scattering occurs, the expected value E is added to the signal, and the corresponding photon packet weight decreases accordingly.

Advantages: Semianalytical MC technology is used to simulate the laser echo signal, and little assumptions are made regarding the photon radiation process; additionally, the obtained simulation results are highly consistent with the actual measurement results.

Disadvantages: The calculation efficiency cannot meet the needs of fast and even real-time calculations in large-scale simulation systems. Table I shows the characteristic statistics of the different simulation models of the laser underwater echo signal.

V. Research Progress on O-LiDAR Echo Signal Modeling and Analysis of Key Factors for Optical Parameter

The current numerical models of LiDAR underwater echo signals are the result of decades of development, range from simple to complex approximations, and include the general LiDAR signal simulation model, the LiDAR signal simulation model based on radiative transfer equation theory, and the LiDAR signal simulation model based on the MC method. Equations (1)–(4) express the solution principles. The parameter information in the analysis formulas (1)–(4) can be summarized qualitatively. The principal factors affecting the backscattered echo signal under the action of the water body when the laser is transmitted in seawater include the following.

The LiDAR system parameters, whose principal influencing factors are as follows.

1) Launch system-related components
   a) Pulse energy

Receiving system related parts

a) Receiving field-of-view (FOV) angle.
b) Receiver aperture.

Emission beam position and attitude

a) LiDAR incidence angle.

1) The water quality optical conditions, whose primary influencing factors are as follows.
   a) Water stratification conditions.
   b) Inherent optical properties.

TABLE I
CHARACTERISTIC STATISTICS OF DIFFERENT SIMULATION MODELS OF LASER UNDERWATER ECHO SIGNAL

LiDAR echo signal acquisition method	Typical transmission model	Transmission model solution method	Advantage	Disadvantage	References
Experience model	Experimental method	Experiment	(1) The result is close to theory;	(1) Requires significant manpower and material resources; larger impact from location and weather factors; not conducive to numerical experiment analysis	Duntley, 1971
Analytical simulation model	Electromagnetic wave theory	Maxwell's equations	(1) Considers the fluctuation principle of photons through laser transmission	(1) Calculating accurate analytical solutions to simplify the above-mentioned equations to the ideal part of the optical transmission conditions is difficult	RL Fante, 1981 Michael I. Mishchenko, 2006
	RadiativeTransfer Equation	Invariant imbedding method	(1) Highly mathematical analysis (2) Including multiple scattering (3) No statistical error in radiation result (4) Fast running speed (running time increases linearly with depth) (5) The most extensive application for solving the radiation equations of water bodies	(1) Difficult to program (2) Solves only one-dimensional problems (one-dimensional refers to the depth information)	Mobley, 1988
		Discrete ordinate method	(1) Accurate irradiance can be obtained with only a small amount of data stream, improving the code execution efficiency (2) Radiation and irradiance can be returned at any optical depth independent of the calculation level (3) Calculates inelastic scattering effect to deal with phenomena such as Raman scattering (4) Includes a wind-blown surface to simulate the basic characteristics of ocean surface roughness	(1) Cannot deal with the high peak scattering phase function well and is not suitable for water with great variation of IOPs with depth (2) Increases the directional dispersion, thereby increasing the amount of calculation	Z.jin, 1994
		Spherical harmonic expansion method	(1)Increase the degree of polynomial expansion to achieve arbitrary accuracy	(1) Difficult to program	EVANS, 1998
Statistical simulation model	Monte Carlo model	Quasi-single-small -angle approximations	(1) Run fast and is robust (2) Uses Fourier transform to obtain precise numerical solutions	(1) The programming algorithm is complex (2) Lengthy solution time	Katsev, 1997 Kim, 2016
		Standard MC simulation	(1) Greatest similarity to the real LiDAR signal transmission process	(1) Low computational efficiency (2) Random error noise	Plass, Kattawar, 1971 Chen, 2020
		Semi-analytical MC simulation	(1) Reduces the statistical uncertainty of the data (2) Improves computational efficiency	(1) Compared with that of the analytical model, the efficiency is not idea	Poole, 1982 Liu, 2020 Zhou,2019

c) The times of photon backward scattering.

2) External environmental conditions, including the primary influencing factors are as follows.
   a) The roughness of the sea surface under driving wind.
   b) Underwater bidirectional reflection distribution function (BRDF) reflection characteristics.

Most O-LiDAR research teams worldwide have conducted in-depth quantitative studies on the three main influencing factors for over nearly half a century. The focus is to summarize and to analyze the effects of LiDAR working height, received field of view angle, water attenuation coefficient, scattering phase function, backscattering number, sea surface roughness, underwater BRDF characteristics, and other factors on the echo signal.

The MC method is close to the real physical transport process of photons and reflects the effect of multiple scattering on the LiDAR return signal. Therefore, the semianalytic MC method—proposed by Pool in 1982—is widely used to quantify the factors affecting the LiDAR echo signal [12], [34], [55], [59]. The factors that can be analyzed using this method include LiDAR system parameters, water quality optical conditions, and external environmental conditions. The system parameters and water optics parameters are primarily determined using the control variable method. During the simulation, the effect of the change in the parameter condition on the laser echo signal can be obtained by changing the size of a parameter in Equation (4) and leaving the other selected parameters unchanged. Quantitative analysis of the effect of the external environment was achieved by optimizing and improving the semianalytic MC boundary judgment conditions. For example, wind-driven changes must be set to the transmission rate of different sea surface roughness values to determine the quality of atmospheric photons passing through water. When the photon reaches the bottom of the water, the conditions must be set according to the reflectivity of the bottom of the water to determine the changes in photon energy and orientation after reflection. When the photon transmission reaches the transmission boundary, the conditions are set by the field of view angle size, receiver aperture size, and other

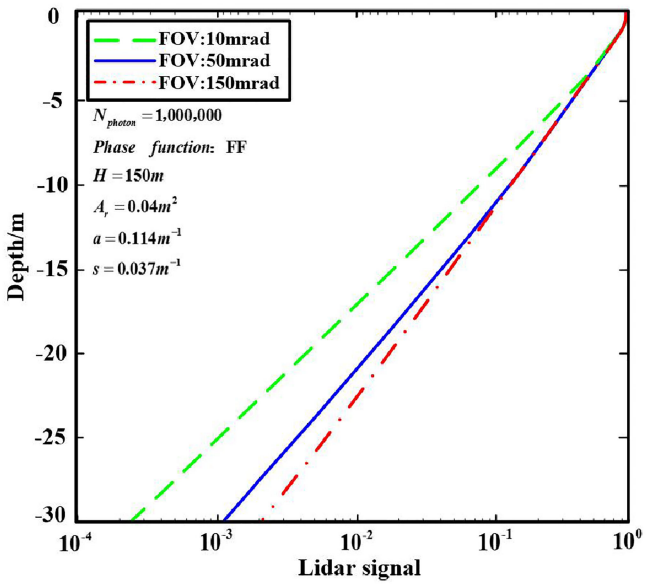

Fig. 2. Semianalytical MC simulation results of echo signals at different FOVs.

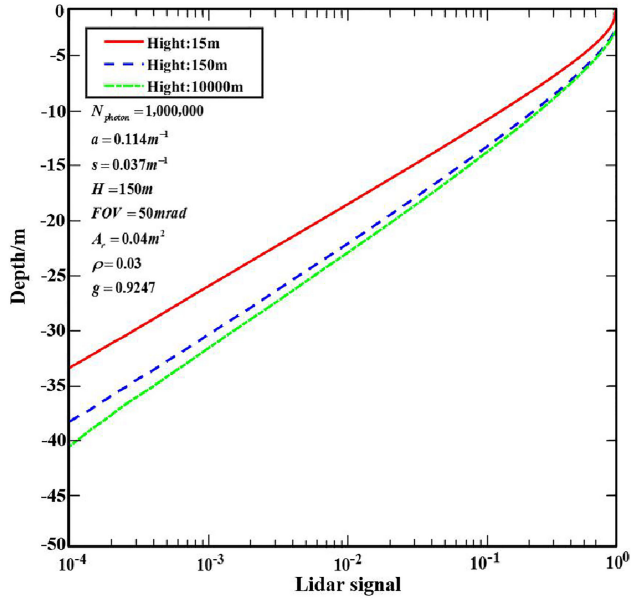

Fig. 3 . Semianalytical MC simulation results of echo signals at different working heights.

parameters to determine whether the photon is within the field of view. The photon then continues transmitting or is declared dead. The number of times the photon is scattered can be set directly in the program, and the change in the return signal under different scattering times can be analyzed.

At present, MC model has widely been used to study the influence of different factors on laser underwater transmission characteristics, for instance [12], [49], [74], [76], [92], [94]. This article refers to the design steps of the semianalytical MC program in [12], [49], [74], [76], [92], [94] to design the semianalytical MC simulation program. When the wavelength is a constant, the energy of the laser pulse is proportional to the number of photons. However, the energy of laser exponentially decays in the water, increasing the laser power, or increasing the number of photons, can increase the ability of measuring depth, but not much. On the other hand, increasing the laser power will increases the power consumption, which affects the measurement time [96]. Semianalytical MC model takes the laser as a huge photon packet, and the number of photons determines the accuracy of simulation results. The number of photons is usually set to approximate $10^5 \sim 10^7$ [33], [76], so, the number of the simulated photons in this article defaults to 10^6.

A. LiDAR System Parameters

1) Effect of Receiver FOV Size on the LiDAR Echo Signal: In this section, the influence of the FOV on the LiDAR underwater echo signal is analyzed using a semianalytical MC model. Fig. 2 shows the simulation results.

The analysis in Fig. 2 shows that the difference in echo signal values obtained by quantization experiments with three different field angles of view (10, 50, and 150 mrad) is different. The signals obtained above 5 m are almost consistent under clean ocean water quality conditions. The echo simulation results obtained from the 50 and 150 mrad FOVs are consistent with the increase in depth. The attenuation rate of the simulated echo signal decreases as the *FOV increases, primarily because the receiver receives multiple scattering echo signals underwater. The experimental results are consistent with the conclusions obtained in [12].

2) Effect of LiDAR Working Height on the LiDAR Echo Signal: In this section, semianalytical MC is used to analyze the influence of LiDAR working height on LiDAR underwater echo signals. Analysis of the simulation results shows that the attenuation rate of the underwater echo signal of the LiDAR decreases with increasing height for LiDAR set at 15, 150, and 10000 m from the water surface (see Fig. 3). This is primarily because the range of received photons corresponding to the field of view angle increases as the height increases; additionally, the number of photons received is greater than that at low working heights. The experimental results are consistent with the conclusions in [12].

B. Water Quality Optical Conditions

The effect of the water quality parameters is generally more important than the effect of LiDAR system parameters (especially the water attenuation coefficient, the single scattering albedo scattering phase function, and stratified water) for analyzing the effect of laser echo signal using the semianalytical MC method.

1) Effect of the Attenuation Coefficient (Homogeneous Water) on the LiDAR Echo Signal: Analyses of the effect of water quality parameters usually use three typical water body optical experimental parameters proposed by Petzold in 1972 [12], [49]. Most experiments show that clean water laser transmission is closer to the quasi-single scattering model, whereas the laser under port water quality is bound to undergo multiple

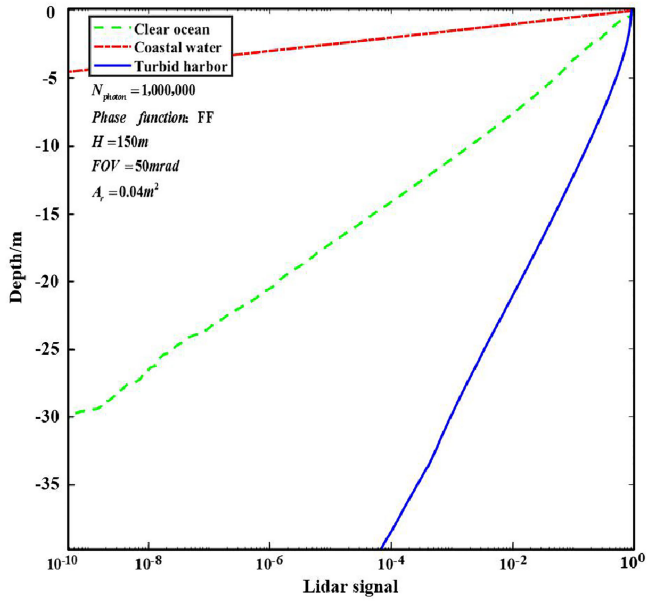

Fig. 4. Semianalytical MC echo signal simulation results under different attenuation coefficients.

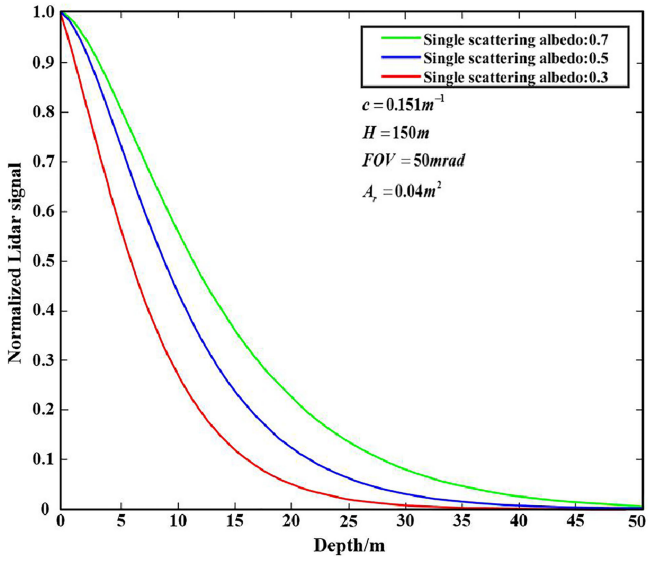

Fig. 5. Simulation echo signal results for different single scattering albedos.

scattering. Larger effective attenuation coefficients of seawater lead to a more significant pulse time expansion.

In this section, a semianalytical MC program is used to simulate the underwater LiDAR echo signals under three typical water conditions. Fig. 4 present the results. The analysis shows that the attenuation rate of the echo signal increases sharply as the water turbidity increases. The laser transmits more than 35 m in ocean clean seawater under the conventional dynamic range of four orders of magnitude. The transmission distance was less than 20 m in coastal seawater. The transport distance in turbid port water was approximately 5 m. Water quality conditions have the most significant influence on laser transmission of the discussed parameters.

2) Effect of Single Scattering Albedo on the LiDAR Echo Signal: The laser echo signal is affected by the single scattering albedo when the attenuation coefficients of the water bodies are equal. In this section assuming that the attenuation coefficients of water bodies are all 0.151m^{-1}. The influence of different single scattering albedos on laser underwater echo signals is analyzed for single-scattering albedos of 0.3, 0.5, and 0.7. Fig. 5 shows the experimental results.

The size of the single scattering albedo determines the proportional relationship between the absorption coefficient and the scattering coefficient. Smaller single scattering albedos of a water body lead to larger absorption coefficients, which increase in absorption and quicken return signal attenuation. The experimental results are consistent with the conclusions in reference [76].

3) Effect of the Scattering Phase Function on the LiDAR Echo Signal: The effect of the scattering phase function on the echo signal and the attenuation coefficient are crucial water column factors. Comparison experiments on the average particle phase function established by Petzold in 1971 through actual measurements have continued uninterrupted since the 1970s [77]–[81]. The selection of the scattering phase function is related to many factors, including water turbidity, suspended particle size and distribution characteristics, the shape of the scattering phase function (which directly affects the determination of the photon scattering angle), and the photon backward scattering process. Therefore, in the process of scattering phase function research, phase functions are often designed close to the Petzold average particle phase function shape and require a flexible scattering angle solution method. For example, in 1994, Fournier and Forand [79] established that a shape of the FF phase function closer to the Petzold phase function than the HG phase function obtained by Kattawar [77] in 1975. However, solving the scattering angle for the phase function is difficult. In 2018, Chen *et al.* [76] established a look-up table method instead of the FF phase function, greatly simplifying the process of solving the scattering angle and improving the computational efficiency of the algorithm.

In this section, the HG phase function, FF phase function, and Petzold phase function are used to simulate the influence of different photon scattering characteristics on LiDAR echo signals for underwater laser transmission. Fig. 6(a) shows that the normalized echo signals obtained by using three phase functions have good consistency. Fig. 6(b) shows that for $g =$ 0.9247, the results obtained by the FF phase function are more consistent with those obtained by the Petzold phase function than those obtained by the HG phase function. Therefore, the phase function is the FF phase function when the semianalytical MC program is used to quantitatively analyze the influence of different factors on the underwater LiDAR echo signal. The experimental results are consistent with the conclusions in [92].

4) Effect of Backscattering Times (Multiple Scattering) on the LiDAR Echo Signal: Since the 1980s, the study of multiple scattering mechanisms has become a global research hotspot. The mainstream single-scattering approximation model can no

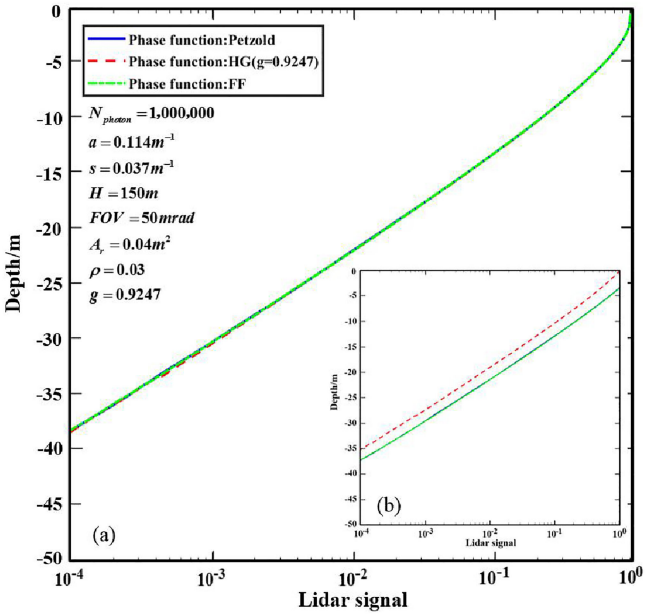

Fig. 6. Simulation results of echo signals under different scattering phase functions. (a) Normalized signal. (b) Nonnormalized signal

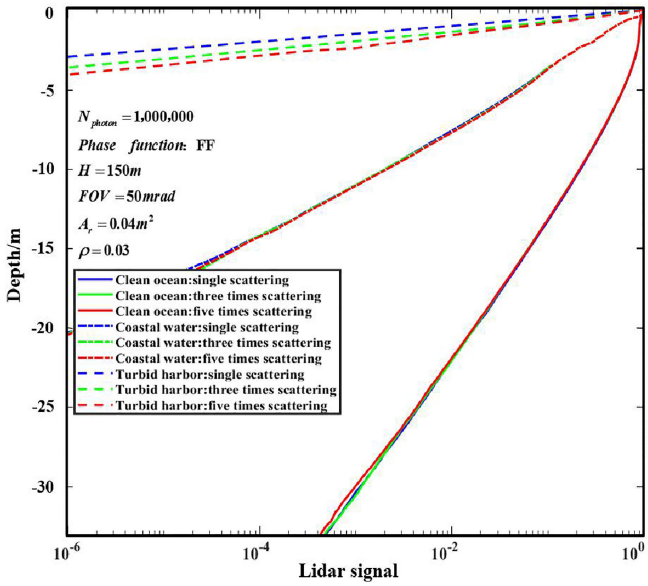

Fig. 7. Simulation results of echo signals under different scattering times.

longer obtain an accurate echo model in a complex water environment. The influencing factors of multiple scattering include LiDAR system parameters and the optical characteristics of the water body. Therefore, studying the effect of multiple scattering on underwater laser transmission can comprehensively analyze the transmission characteristics. MC simulations are primarily used as research methods [12], [49], [76]. For example, Chen *et al.* [94] simulated the echo signal using the semianalytical MC method. The single, secondary, tertiary, and higher degrees were simulated.

In this section, a semianalytical MC program is used to simulate the influence of different backscattering times on the underwater transmission of a LiDAR echo signal in three typical water bodies. Fig. 7 presents the results. The analysis shows little difference between the results of multiple and single scattering in clean water conditions. However, in turbid water, the attenuation rate of multiple scattering echo signals is smaller than that of single-scattering echo signals. Thus, the principle of the widely used "single backscattering approximation" is satisfied in clean water when the laser propagates underwater. The scattering coefficient of turbid water increases, making photons more prone to multiple backscattering. Therefore, the single scattering approximation theory cannot be used in underwater LiDAR transmission experiments in coastal waters; however, the influencing factors of multiple scattering must be considered.

5) Effect of Stratified Water on LiDAR Echo Signal: In the above analysis of the influence of different factors on the laser echo signal underwater transmission assumed homogeneous water quality parameters in the vertical direction.

The changing vertical profile concentrations of the phytoplankton layer and the profile of the water attenuation coefficient are affected by the density distribution of suspended matter and turbulence in the coastal water body. The key to analyzing the effect of stratified water on echo signals using the MC method is to establish a functional model of the water attenuation coefficient with depth change. For example, the bio-optical model [36] from 1982 represents the change in the water attenuation coefficient under the effect of chlorophyll concentration with depth change. Therefore, in the 1980s, the relationship between chlorophyll concentration and the water attenuation coefficient was deeply studied. In 1983, Lewis *et al.* [82] first used a Gaussian distribution function to express the distribution law of chlorophyll concentration with water depth. In 1991, Morel [91] introduced an analytical relationship between the absorption coefficient, the scattering coefficient, and the chlorophyll concentration distribution in case 1 water. This relationship is widely used to determine the attenuation coefficients of stratified water [74]. Researchers have since quantitatively analyzed the effect of the chlorophyll concentration and water attenuation coefficient function on laser underwater transmission using an echo signal simulation model. In 1992, Gordon [83] used a MC numerical model to analyze stratified water according to the vertical structure of chlorophyll. In 2019, Chen *et al.* [94] used a semianalytical MC method to simulate the LiDAR echo signals of a laser in homologous and stratified water. In the simulation, a Gaussian phytoplankton distribution model was used to simulate the distribution change in chlorophyll concentration with depth.

This section uses the bio-optical model in [74] and the semianalytical MC program to simulate the echo signals transmitted by the laser in heterogeneous water under different chlorophyll concentration distribution center depths (5, 10, 15, and 25 m). Fig. 8 shows the results. The analysis shows that when the absorption coefficient and scattering coefficient of the water body changed with the water body resolution, the echo signal obtained by simulation will no longer satisfy the exponential decay law.

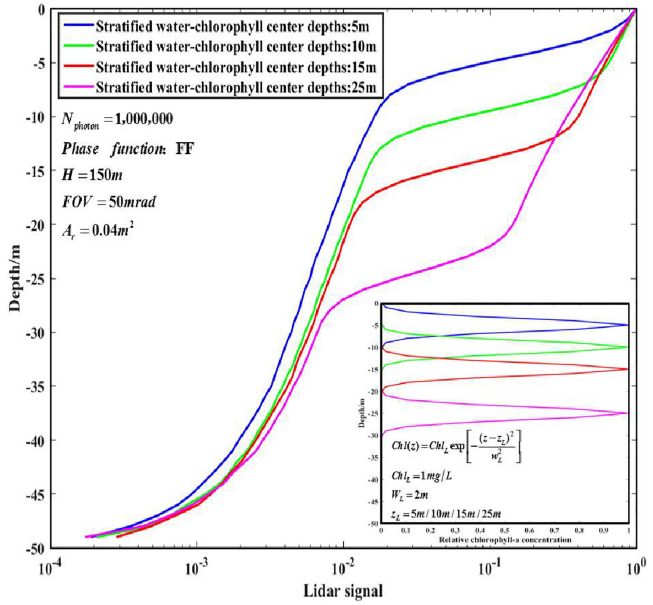

Fig. 8. Effect of heterogeneous water body on the echo signal

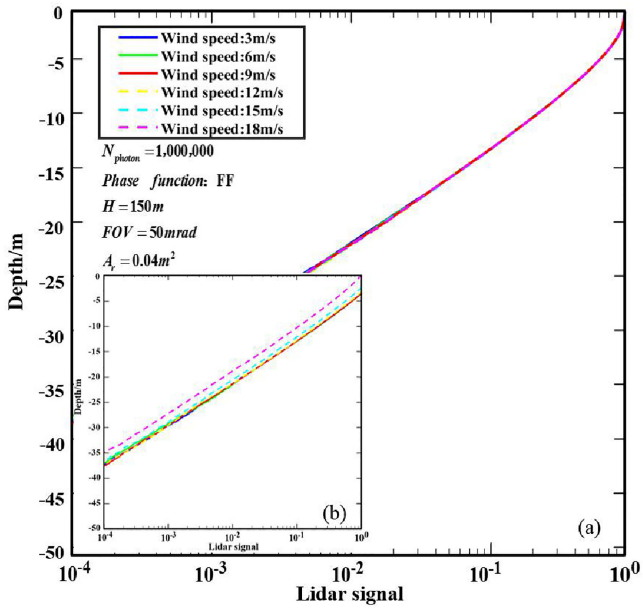

Fig. 9. Variation of air-sea interface transmittance on a rough sea surface with different wind speeds. (a) Normalized signal. (b) Nonnormalized signal.

The laser echo simulation signal will be large fluctuations near the peak of the chlorophyll a concentration.

C. External Environmental Conditions

1) Effect of Wind-Driven Rough Sea Surface on the LiDAR Echo Signal: The effect of a rough sea surface on laser transmission can be summarized as an external environmental factor. In 1954, Cox and Munk [85] studied the relationship between the mean square value σ_m of sea surface slope distribution and wind speed v. Under the effect of wind, waves and bubbles were generated on the calm sea surface; the relationship between foam coverage k_s and wind speed v can be expressed by the Monahan function model [86]. According to the sea surface transmittance as the product of calm and foamy sea surface transmittances, the change in laser transmittance on the sea surface with the change in wind speed can be calculated. The theory quantifies the change in rough sea surface transmittance under different wind speeds. Therefore, researchers have widely used the MC model to quantitatively analyze the effect of rough sea surfaces on echo signals. According to formula (4), the quantitative analysis of this factor is based on the design of MC boundary conditions. The transmittance of the sea surface determines the number of passing photons, which affects echo signal formation. For example, in 1992, Kargin *et al.* [87] analyzed the formation of LiDAR signals affected by wind-driven rough sea surfaces. In 2005, Kokhanenko [88] used the MC method to analyze the combined effect of multiple scattering and wind-driven sea waves on the LiDAR sensing results of upper seawater layers. The effect of wind-driven waves causes the decay rate of the singly scattered radiation power to increase with depth. In 2018, Chen *et al.* [76] found that laser beam transmittance has a significant relationship with the incident angle and wind speed.

This section uses the analytical relationship between sea surface transmittance and wind speed in [76] and the semianalytical MC program to simulate the echo signals transmitted by the laser at six different wind speeds (3, 6, 9, 12, 15, and 18 m/s). Fig. 9(a) shows that the normalized echo signals obtained by different wind speeds have good consistency. The analysis in Fig. 9(b) shows that the change in transmittance has little effect on the laser underwater echo signal when considering only the influence of wind speed on the transmittance for wind speeds below 9 m/s; further, at wind speeds greater than 12 m/s, the attenuation value of the laser underwater echo signal increases as the wind speed changes. The experimental results are consistent with the conclusions in [76]. Additionally, the influence of the rough sea surface on the underwater laser transmission is related to the laser incident angle. Chen *et al.* [76] showed that incident angles of less than 30° had little effect on the transmittance of the blue-green laser. Moreover, most of the light is refracted into the seawater. The transmittance decreases slowly as the incident angle increases from 30° to 60° and decreases sharply as the incident angle increases from 60° to 90°. When the laser is transmitted from seawater to the atmosphere, the laser transmittance is strongly related to the incident angle and the wind speed. Because the refractive index of seawater is larger than that of air, total reflection may occur. The critical angle of total reflection is approximately 48°, and the transmittance after total reflection is almost zero. For incident angles of less than 20°, the transmittance is basically unchanged. The transmittance decreases linearly as the incident angle increases from 20° to 35° and decreases sharply as the incident angle increases beyond 35°.

2) Effect of Sea Bottom BRDF Characteristics on the LiDAR Echo Signal: The reflectivity property of water bottom is one of the boundary conditions in the process of laser propagation in

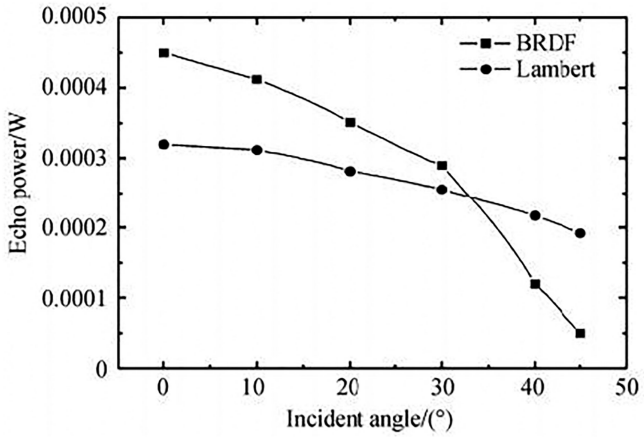

Fig. 10. Variation law of the echo signal under different incident angles of different bottom sediment characteristics [89].

water, and the BRDF property of water bottom determines the distribution of reflectivity of water bottom. The characteristics of sea bottom BRDF are also classified as external factors that correspond to setting boundary conditions in the quantitative analysis. Setting the water depth requires calculating the change in photon energy and transmission orientation upon reaching the underwater boundary according to the sea bottom BRDF characteristics. The widely used design of the sea bottom surface as a Lambert characteristic surface is inconsistent with actual physical transmission process. For non-Lambert surfaces, the BRDF is widely used worldwide to express the reflection characteristics of the target surface in space for different incident angles. For example, Zhang *et al.* [90] measured the BRDF characteristics of underwater sediment and aquatic plants in 2003 and found that the BRDF is similar to Lambert characteristics for incident angles less than 35°. In contrast, significant backscattering in the zenith angle direction with a brightness value several times greater than that at other angles increases significantly as the incident angle increases. Tan *et al.* [89] used the MC method in 2016 to simulate the reflection characteristics of underwater targets by replacing Lambert characteristics with a six-parameter BRDF model (in addition to the Rahman model). The echo characteristics of the laser reflection were simulated by the sampling method. Simulations and experiments were conducted on the target echoes at different incident angles at the same distance. The simulation results were compared with the simulation and experimental results based on the Lambert surface reflection sampling method. Fig. 10 presents the experimental results. The target echo simulated by considering BRDF characteristics is stronger than the simulation result based on Lambert surface reflection sampling for small incident angles; however, as the incident angle increases, the BRDF simulation result decreases rapidly. For incident angles greater than 30°, the BRDF result is smaller than the simulation result based on Lambert surface reflection sampling. Comparing the two simulation methods with the laboratory results revealed that with the change in the incident angle and the variation law of the target echo amplitude obtained by the MC simulation is basically consistent with the experimental results.

TABLE II
SUMMARY OF THE INFLUENCES OF DIFFERENT FACTORS ON THE UNDERWATER LASER ECHO SIGNAL

Primary factor	Representative influencing factors	Effect content
LiDAR system parameters	FOV	(1) The attenuation rate of the simulated echo signal decreases as the FOV increases (2) Smaller receiving angles limit the reception of multiple scattered signals (3) The LiDAR signal converges to the "single scattering approximation" of the LiDAR equation
	Height	(1) Lower working heights produce faster signal attenuation (2) The range of received photons corresponding to the field of view angle increases as the height increases (3) The number of photons received is greater than that at a low working heights
Water optical property	Attenuation coefficient	(1) The attenuation rate of the echo signal increases sharply as the water turbidity increases (2) Water quality conditions have the most significant influence on laser transmission of the discussed parameters
	Single scattering albedo	(1) Smaller single scattering albedos of a water body lead to larger absorption coefficients, which increase in absorption and quicken return signal attenuation
	Scattering phase function	(1) Affects the determination of the photon scattering angle, and the photon backward scattering process (2) The FF phase function are more consistent with those obtained by the Petzold phase function than those obtained by the HG phase function
	Multiple scattering	(1) The analysis shows little difference between the results of multiple and single scattering in clean water conditions (2) In turbid water, the attenuation rate of multiple scattering echo signals is smaller than that of single-scattering echo signals
External environmental conditions	Stratified Water	(1) The echo signal obtained by simulation will no longer satisfy the exponential decay law (2) The laser echo simulation signal will be large fluctuations near the peak of the chlorophyll a concentration
	Wind-driven Rough Sea Surface	(1) The laser beam transmittance has a strong relationship with the incident angle and wind speed
	Sea bottom BRDF Characteristics	(1) The target echo simulated by considering BRDF characteristics is stronger than the simulation result based on Lambert surface reflection sampling for small incident angles (2) For incident angles greater than 30°, the BRDF result is smaller than the simulation result based on Lambert surface

Table II gives a summary of the influence characteristics of different factors on the underwater laser echo signal.

VI. CONCLUSION

O-LiDAR technology has been developed for more than 50 years. Mainstream mature commercial products are widely used in military and civil fields, such as underwater geomorphology mapping, hydrological parameter telemetry, and marine environmental pollution monitoring. Compared with costly field experimental research, the simulation modeling theory of the LiDAR

water echo signal and the theory of retrieving water optical parameters using LiDAR water echo signals have developed into an important research direction worldwide. This article began by addressing the formation principle of laser LiDAR underwater transmission echo signals and comprehensively summarized the current laser LiDAR echo signal simulation modeling theory; the primary influencing factors of echo signal simulation; and the principal methods, which include the following.

1) Formation principle of the LiDAR echo signal can be described by the LiDAR equation approximating single scattering. This method has been widely used, but has limitations for quantitatively analyzing the effect of the water quality environment, the LiDAR parameters, and external conditions on echo signals. Accurately describing the effect of seawater on multiple laser scattering is particularly difficult. In addition, researchers primarily simulate high-precision water LiDAR echo signals using models due to the high cost of field measurement experiments.
2) LiDAR echo signal simulation models are primarily established using analytical and statistical methods. According to photon characteristics, different analytical methods include theory for Maxwell's equations based on the wave characteristics of light and radiation transfer theory of the particle characteristics of light. Because of the need to establish a high-precision simulation model that can describe the multiple scattering of laser in water, the radiation transfer theory is usually used with the analytical method to create an echo signal simulation model. Because solving the radiation transfer equation established by this method is difficult, the approximate solution in the radiation transfer theory can be obtained by using the small-angle approximation theory and Fourier transform by considering the geometric characteristics of laser underwater transmission. The theoretical results are used as the current mainstream analytical echo signal simulation model. The statistical model is more widely used than the high-solution-efficiency analytical model due to its better approximation of the real physical process of laser propagation in water. The development of this theory primarily includes the standard MC method and the semianalytical MC method. The semianalytical MC method has higher accuracy and efficiency than the standard MC method in the simulation process.
3) Factors affecting the simulation accuracy of the echo signals are primarily a function of the LiDAR system parameters, water optical parameters, and the external environment. We summarized and analyzed the effects of LiDAR working height, receiver field of view angle, water attenuation coefficient, scattering phase function, single scattering albedo, backscattering times, stratified water, rough sea surface driven by wind and incident angle, and sea bottom BRDF characteristics on echo signals according to the control variable method. The summary of the experimental results found that water quality has the greatest influence on LiDAR echo signals of the three influencing factors. The attenuation rate of the echo signal increased sharply as the water turbidity increased. In addition, the attenuation rate of the LiDAR echo signal decreased as the LiDAR working height and field of view angle increased. The attenuation rate of the echo signal increased as the single scattering albedo decreases when the attenuation coefficient of the water body was equal. The echo signal simulated by the FF phase function was closer to the Petzold average phase function than to the HG and FF phase functions. The selection of the phase function is very important in the simulation model. The most important of the many factors affecting the multiple scattering effects of LiDAR underwater echo signals is the water attenuation coefficient. In clean water, the multiple scattering effects are not significant; and the echo signal conforms to the principle of "single backscattering approximation." However, the influence of multiple scattering on echo signals becomes increasingly obvious as the water turbidity increases. Laser underwater transmission approximates the exponential attenuation law in a uniform water body; however, actual water bodies are mostly stratified. The attenuation rate of the echo signal changes according to the change in the water body attenuation coefficient in a stratified water body, which no longer conforms to the exponential attenuation law. The formation of stratified water is mostly related to the distribution of chlorophyll concentration. Waves and bubbles form on rough sea surfaces and affect the transmittance and reflectivity of laser propagation at the air-water interface. Wind is the primary driving factor for the formation of rough water surfaces. Thus, exploring the influence of rough water surfaces on the transmittance driven by different wind speeds is essential. The characteristics of the sea bottom BRDF determine the reflection process of the laser after reaching the underwater boundary. The introduction of the sea bottom BRDF characteristic model yields a more accurate underwater echo signal simulation model than the current Lambert characteristic assumptions.

Progress has been made in O-LiDAR radiation transmission modeling, echo signal simulation, and echo signal effect mechanism; however, deficiencies in the key transmission links, the multiple scattering effect, and the O-LiDAR detection mechanism require more detailed research. The development of O-LiDAR technology continues improving the performance of related hardware facilities, detection accuracy, and efficiency. Further, the functions and forms of LiDAR are constantly enriched. The higher precision detection of optical water body parameters is the principal development direction of O-LiDAR in the future. Additional areas of future research include the underwater propagation characteristics of lasers, quantitative analysis of the energy attenuation characteristics of laser propagation with seawater turbulence, inelastic scattering (Raman scattering), laser polarization, and BRDF characteristics of rough water surface and underwater sediment. Here, a research system combining LiDAR theory and experiments was developed to provide sufficient theoretical guidance for the subsequent development of LiDAR ocean measurement experiments and to verify the

current theoretical research by using the subsequent experimental results to effectively evaluate and to verify the underwater transmission characteristics of LiDAR and the accuracy of detecting the optical characteristics of water bodies. We predict that O-LiDAR technology will strongly support a deeper human understanding of the ocean.

REFERENCES

[1] S. Sizgoric, J. Banic, and G. C. Guenther, "1970–1990: Airborne LiDAR hydrography status," *EARSeL Adv. Remote Sens.*, vol. 1, pp. 95–101, 1992.

[2] Tsai-Chen Wu *et al.*, "Blue laser diode enables underwater communication at 12.4Gbps," *Sci. Rep.*, vol. 7, no. 6, 2017, Art. no. 40480.

[3] G. D. Hickman and J. E. Hogg, "Application of an airborne pulsed laser for near shore bathymetric measurements," *Remote Sens. Environ.*, vol. 1, no. 1, pp. 47–58, 1969.

[4] G. Zhou and M. Xie, "Coastal 3-D morphological change analysis using LiDARSeries data: A case study of assateague island national seashore," *J. Coastal Res.*, vol. 25, no. 2, pp. 435–447, 2009.

[5] Y. Pastol, "Use of airborne LiDAR bathymetry for coastal hydrographic surveying: The French experience," *J. Coastal Res.*, vol. 62, no. 2, pp. 6–18, 2011.

[6] G. Zhou and X. Zhou, *Urban High-Resolution Remote Sensing: Algorithms and Modelling*. New York, NY, USA: Taylor & Francis, 2020.

[7] G. Zhou and X. Zhou, "Seamless fusion of LiDAR and aerial imagery for building extraction," *IEEE Trans. Geosci. Remote Sens.*, vol. 52, no. 11, pp. 7393–7407, Nov. 2014.

[8] G. Zhou, C. Song, J. Simmers, and P. Cheng, "Urban 3D GIS from LiDAR and digital aerial images," *Comput. Geosci.*, vol. 30, no. 4, pp. 345–353, 2004.

[9] T. Dickey, M. Lewis, and G. Chang, "Optical oceanography: recent advances and future directions using global remote sensing and in situ observations," *Rev. Geophys.*, vol. 44, no. 1, 2006, Art. no. RG1001.

[10] C. A. Hostetler *et al.*, "Spaceborne lidar in the study of marine systems," *Annu. Rev. Marine Sci.*, vol. 10, no. 1, pp. 121–147, 2018.

[11] G. Zhou, *et al.*, "Design of supercontinuum laser hyperspectral light detection and ranging (LiDAR) (SCLaHS LiDAR)," *Int. J. Remote Sens.*, vol. 42, no. 10, pp. 3731–3755, 2021.

[12] Y. Zhou, *et al.*, "Validation of the analytical model of oceanic lidar returns: Comparisons with Monte Carlo simulations and experimental results," *Remote Sens.*, vol. 11, no. 16, pp. 1870–1887, 2019.

[13] H. C. Van de Hulst and V. Twersky, "Light scattering by small particles," *Phys. Today*, vol. 10, no. 12, pp. 28–30, 1957.

[14] G. D. Hickman and J. E. Hogg, "Application of an airborne pulsed laser for near shore bathymetric measurements," *Remote Sens. Environ.*, vol. 1, no. 1, pp. 47–58, 1969.

[15] S. Duntley, *Underwater Lighting by Submerged Lasers and Incandescent Sources*. San Diego, CA, USA: Scripps Inst. Oceanography Visibility Lab., Jun. 1971.

[16] R. W. Preisendorgfer *et al.*, *Radiative Transfer on Discrete Spaces*. Oxford, U.K.: Pergamon Press, 1965.

[17] G. P. Sorenson, R. C. Honey, and J. R. Payne, "Analysis of the use of airborne laser radar of submarine detection and ranging," Stanford Res. Inst., Menlo Park, CA, USA, SRI Report No. 5583, 1966.

[18] G. N. Plass and G. W. Kattanwar, "Monte Carlo Calculations of light scattering from clouds," *Appl. Opt.*, vol. 7, no. 3, 1968, Art. no. 415.

[19] D. G. Collins and M. B. Wells, "Monte Carlo codes for the study of light transport in the atmosphere," Radiation Res. Assoc., Inc., Fort Worth, TX, USA, 1965.

[20] D. G. Collins, K. Cunningham, and M. B. Wells, "Monte Carlo studies of light transport," Radiation Res. Assoc. Inc., Fort Worth, TX, USA, Report RRA-T74, 1967.

[21] K. Saylam, "Airborne lidar bathymetry: Assessing quality assurance and quality control methods with Leica Chiroptera examples," *Int. J. Remote Sens.*, vol. 39, no. 8, pp. 2518–2542, 2018.

[22] A. I. Bruscaglioni and G. Zaccanti, "Monte-Carlo calculations of LIDAR returns: Procedure and results," *Appl. Phys. B.*, vol. 60, no. 4, pp. 325–329, 1995.

[23] D. M. Winker and L. R. Poole, "Monte-Carlo calculations of cloud returns for ground-based and space-based LIDARS," *Appl. Phys. B*, vol. 60, no. 4, pp. 341–344, 1995.

[24] A. V. Starkov z, M. Noormohammadian, and U. G. Oppel, "A stochastic model and a variance-reduction Monte-Carlo method for the calculation of light transport," *Appl. Phys. B*, vol. 60, no. 4, pp. 335–340, 1995.

[25] P. F. Schippnick, "Phenomeno logical model of beam spread in ocean water," *Oceanic Opt. X*, vol. 26, no. 6, pp. 561–565, 1990.

[26] T. J. Petzold, "Volume scattering functions for selected ocean waters," 1972.

[27] H. T. Yura, "Small-angle scattering of light by ocean water," *Appl. Opt.*, vol. 10, no. 1, pp. 114–118, 1971.

[28] Daniel T. Gillespie, "Stochastic-analytic approach to the calculation of multiply scattered lidar returns," *J. Opt. Soc. Amer. A*, vol. 2, no. 8, pp. 1307–1324, 1985.

[29] D. Arnush, "Underwater light-beam propagation in the small-angle-scattering approximation," *J. Opt. Soc. Amer.*, vol. 62, no. 9, pp. 1109–1111, 1972.

[30] L. B. Stotts, "Closed form expression for optical pulse broadening in multiple-scattering media," *Appl. Opt.*, vol. 17, no. 4, 1978, Art. no. 504.

[31] R. F. Lutomirski, "An analytic model for optical beam propagation through the marine boundary layer," in *Proc. Oceanic Opt.*, 1978, pp. 110–122.

[32] R. L. Fante, "Relationship between radiative-transport theory and Maxwell's equations in dielectric media," *J. Opt. Soc. Amer.*, vol. 71, no. 4, pp. 460–468, 1981.

[33] L. R. Poole, D. D. Venable, and J. W. Campbell, "Semianalytic Monte Carlo radiative transfer model for oceanographic lidar systems," *Appl. Opt.*, vol. 20, no. 20, pp. 3653–3656, 1981.

[34] L. R. Poole, "Computed laser backscattering from turbid liquids: comparison with laboratory results," *Appl. Opt.*, vol. 21, no. 12, pp. 2262–2264, 1982.

[35] H. R. Gordon, "Interpretation of airborne oceanic lidar: effects of multiple scattering," *Appl. Opt.,* vol. 21, no. 16, pp. 2996–3001, 1982.

[36] K. S. Baker and R. C. Smith, "Bio-optical classification and model of natural waters," *Limnol. Oceanogr.*, vol. 27, no. 3, pp. 500–509, 1982.

[37] K. Stamnes, "The theory of multiple scattering of radiation in plane parallel atmospheres," *Rev. Geophys.*, vol. 24, no. 2, pp. 299–310, 1986.

[38] Mobley and B. Preisendorfer, "The principal discriminant method of prediction: Theory and evaluation," *J. Geophys. Res.*, vol. 93, pp. 10815–10830, 1988.

[39] H. R. Gordon, "Can the Lambert-Beer law be applied to the diffuse attenuation coefficient of ocean water?," *Limnol. Oceanogr.*, vol. 34, no. 8, pp. 1389–1409, 1989.

[40] L. Wang, S. L. Jacqes, and L. Zheng, "MCML—Monte Carlo modeling of light transport in multi-layered tissues," *Comput. Meth. Program. Biol.*, vol. 47, no. 2, pp. 131–146, 1995.

[41] I. L. Katsev *et al.*, "Efficient technique to determine backscattered light power for various atmospheric and oceanic sounding and imaging systems," *J. Opt. Soc. Amer. A.,* vol. 14, no. 6, pp. 1338–1346, 1997.

[42] C. Acquista and J. L. Anderson, "A derivation of the radiative transfer equation for partially polarized light from quantum electrodynamics," *Ann. Phys.*, vol. 106, no. 2, pp. 435–443, 1977.

[43] R. E. Walker and J. W. McLean, "Lidar equations for turbid media with pulse stretching," *Appl. Opt.*, vol. 38, no. 12, pp. 2384–2397, 1999.

[44] G. M. Krekov *et al.*, "Laser sensing of a subsurface oceanic layer," *Appl. Opt.*, vol. 37, no. 9, pp. 1589–1595, 1998.

[45] M. Gimond, "Description and verification of an aquatic optics Monte Carlo model," *Environ. Model. Softw.*, vol. 19, no. 12, pp. 1065–1076, 2004.

[46] Y. I. Kopilevich *et al.*, "Mathematical modeling of input signals for oceanographic lidar systems," *Proc. SPIE*, vol. 5155, pp. 30–39, 2003.

[47] H. Abdallah, "Wa-LiD: A new LiDAR simulator for waters," *IEEE Geosci. Remote Sens. Lett.*, vol. 9, no. 4, pp. 744–748, Jul. 2012.

[48] E. E. Perez Mayesffer *et al.*, "3D Monte Carlo analysis on photons step through turbid medium by Mie scattering," *Revista Mexicana de Fisica*, vol. 67, no. 2, pp. 292–298, 2021.

[49] Q. Liu *et al.*, "A semianalytic Monte Carlo simulator for spaceborne oceanic LiDAR: Framework and preliminary results," *Remote Sens.*, vol. 12, no. 17, pp. 2820–2835, 2020.

[50] M. Kim *et al.*, "Modeling of airborne bathymetric lidar waveforms," *J. Coastal Res.*, vol. 76, pp. 18–30, 2016.

[51] F. Voit *et al.*, "Multiple scattering of polarized light: comparison of Maxwell theory and radiative transfer theory," *J. Biomed. Opt.*, vol. 17, no. 4, 2012, Art. no. 045003.

[52] L. G. Sokoletsky *et al.*, "A comparison of numerical and analytical radiative-transfer solutions for plane albedo of natural waters," *J. Quant. Spectrosc. Radiat. Transf.*, vol. 110, no. 12, pp. 1132–1146, 2009.

[53] I. Michael, "Mishchenko "Maxwell's equations, radiative transfer, and coherent backscattering: A general perspective," *J. Quant. Spectrosc. Radiat. Transf.*, vol. 101. no. 3, pp. 540–555, 2006.
[54] J. H. Churnside, "Review of profiling oceanographic lidar," *Opt. Eng.*, vol. 53, no. 5, pp. 1–13, 2014.
[55] D. Liu, *et al.*, "Lidar remote sensing of seawater optical properties: experiment and Monte Carlo simulation," *IEEE Geosci Remote Sens.*, vol. 57, no. 11, pp. 9489–9498, Nov. 2019.
[56] A. P. Vasilkov *et al.*, "Airborne polarized lidar detection of scattering layers in the ocean," *Appl. Opt.*, vol. 40, no. 24, pp. 4353–4364, 2001.
[57] C. D. Mobley *et al.*, "Comparison of numerical models for computing underwater light fields," *Appl. Opt.*, vol. 32, no. 36, pp. 7484–7504, 1993.
[58] I. V. Samokhvalov, "Double-scattering approximation of lidar equation for inhomogeneous atmosphere," *Opt. Lett.*, vol. 4, no. 1, pp. 12–14, 1979.
[59] M. Gimond, "Description and verification of an aquatic optics Monte Carlo model," *Environ. Model. Softw.*, vol. 19, no. 12, pp. 1065–1076, 2004.
[60] C. Mobley, "A numerical model for the computation of radiance distributions in natural waters with wind-roughened surfaces," *Limnol. Oceanogr.,* vol. 34, pp. 1473–1483, 1989.
[61] C. Mobley and R. Preisendorfer, "A numerical model for the computation of radiance distributions in natural waters with wind-roughened surfaces," *Limnol. Oceanogr.*, vol. 34, pp. 1473–1483, 1988.
[62] D. Contini, F. Martelli, and G. Zaccanti, "Photon migration through a turbid slab described by a model based on diffusion approximation I. Theory," *Appl. Opt.*, vol. 36, no. 19, pp, 4587–4599, 1997.
[63] Z. Jin and K. Stamnes, "Radiative transfer in nonuniformly refracting layered media such as the atmosphere-ocean system," *Appl. Opt.*, vol. 33, no. 3, pp. 431–422, 1994.
[64] K. Stamnes and R. A. Swanson, "A new look at the discrete ordinate method for radiative transfer calculations in anisotropically scattering atmospheres," *J. Atmos. Sci.* vol. 38, pp. 387–399, 1981.
[65] K. Stamnes and H. Dale, "A new look at the discrete ordinate method for radiative transfer calculations in anisotropically scattering atmospheres II: Intensity computations," *J. Atmos. Sci.*, vol. 38, pp. 2696–2706, 1981.
[66] K. Stamnes, S. C. Tsay, W. Wiscombe, and K. Jayaweera, "Numerically stable algorithm for discrete-ordinate-method radiative transfer in multiple scattering and emitting layered media," *Appl. Opt.* vol. 27, pp. 2502–2509, 1988.
[67] K. Mitra and J. H. Churnside, "Transient radiative transfer equation applied to oceanographic lidar," *Appl. Opt.*, vol. 38, no. 6, pp. 889–895, 1999.
[68] Y. A. Ilyushin1 and V. P. Budak, "Narrow beams in scattering media: the advanced small-angle approximation," *J. Opt. Soc. Amer. A*, vol. 28, no. 7, pp. 1358–1363, 2011.
[69] C. D. Mobley, "Hydrolight 3.1 Users' guide," SRI Int., Menlo Park, CA, USA, 6583FR, 1996.
[70] G. P. Anderson *et al.*, "Reviewing atmospheric radiative transfer modeling: new developments in high- and moderate-resolution FASCODE/FASE and MODTRAN," *Proc. SPIE*, vol. 2830, pp. 82–93, 1996.
[71] K. F. Evans, "The spherical harmonics discrete ordinate method for three-dimensional atmospheric radiative transfer," *J. Atmos. Sci.*, vol. 55, no. 3, pp. 429–446, 1998.
[72] M. Lukáčová-Medvid'ová and Z. Vlk, "Well-balanced finite volume evolution Galerkin methods for the shallow water equations with source terms," *Int. J. Numer. Method FL*, vol. 47, no. 10/11, pp. 1165–1171, 2005.
[73] L. R. Bissonnette, "Lidar and multiple scattering," in *Lidar: Range-Resolved Optical Remote Sensing of the Atmosphere*. C. Weitkamp, Ed., New York, NY, USA: Springer, 2005, pp. 43–103.
[74] Q. Liu *et al.*, "Relationship between the effective attenuation coefficient of spaceborne lidar signal and the IOPs of seawater," *Opt. Exp.*, vol. 26, no. 23, pp. 30278–30291, 2018.
[75] A. Kokhanovsky, "Small-angle approximations of the radiative transfer theory," *J. Phys. D, Appl. Phys.*, vol. 30, pp. 2837–2840, 1997.
[76] P. Chen, D. Pan, Z. Mao, and H. Liu, "Semi-analytic monte carlo model for oceanographic lidar systems: Lookup table method used for randomly choosing scattering angles," *Appl. Sci.*, vol. 9, no. 1, pp. 48–60, 2018.
[77] G. W. Kattawar, "A three-parameter analytic phase function for multiple scattering calculations," *J, Quant. Spectrosc Radiat. Transf.*, vol. 15, no. 9, pp. 839–849, 1975.
[78] W. M. Cornette and J. G. Shanks, "Physically reasonable analytic expression for the single-scattering phase function," *Appl. Opt.*, vol. 31, no. 16, pp. 3152–3160, 1992.
[79] G. R. Fournier and J. L. Forand, "Analytic phase function for ocean water," *SPIE Oceanic Opt. XII*, vol. 2258, pp. 194–201, 1994.
[80] V. I. Haltrin, "Theoretical and empirical phase functions for Monte Carlo calculations of light scattering in seawater," in *Proc. 4th Int. Conf. Remote Sens. Marine Coastal Environ.*, 1997, vol. I, pp. I-509–I-518.
[81] S. Sahu, "Semi-analytical modeling and parameterization of particulates-in-water phase function for forward angles," *Opt. Exp.*, vol. 23, no. 17, pp. 22291–22307, 2015.
[82] M. R. Lewis, J. J. Cullen, and T. Platt, "Phytoplankton and thermal structure in the upper ocean: Consequences of nonuniformity in chlorophyll profile," *J. Geophys. Res.*, vol. 88, pp. 2565–2570, 1983.
[83] H. R. Gordon, "Diffuse reflectance of the ocean: Influence of nonuniform phytoplankton pigment profile," *Appl. Opt.* vol. 31, no. 12, pp. 2116–2129, 1992.
[84] G. Zhou, X. Zhou, J. Yang, Y. Tao, X. Nong, and O. Baysal, "Oktay baysal, flash lidar sensor using fiber coupled APDs," *IEEE Sensor J.*, vol. 15, no. 9, pp. 4758–4768, Sep. 2015.
[85] C. Cox and W. Munk, "Measurement of the roughness of the sea surface from photographs of the Sun's Glitter," *J. Opt. Soc. Amer.*, vol. 44, no. 11, pp. 838–850, 1954.
[86] E. C. Monahan, D. E. Spiel, and K. L. Davidson, "A model of marine aerosol generation via whitecaps and wave disruption," *Oceanic Whitecaps*, vol. 2, pp 167–174, 1986.
[87] B. A. Kargin, G. M. Krekov, and M. M. Krekova, "Influence of water surface roughness on lidar return characteristics," *Atmos. Ocean. Opt.*, vol. 5, no. 3, pp. 292–299, 1992.
[88] G. P. Kokhanenko *et al.*, "Influence of the air–water interface on hydrosol lidar operation," *Appl. Opt.*, vol. 44, no. 17, pp. 3510–3519, 2005.
[89] Y. Tan, H. Zhang, and B. Zha, "Simulation of underwater laser fuze echo based on bidirectional reflectance distribution function," *Acta Phtonica Sinica*, vol. 45, no. 12, pp. 59–64, 2016.
[90] H. Zhang *et al.*, "Bidirectional reflectance measurements of sediments in the vicinity of Lee Stocking Island, Bahamas," *Limnol. Oceanogr.*, vol. 48, no.1, pp. 380–389, 2003.
[91] A. Morel, "Light and marine photosynthesis: a spectral model with geochemical and climatological implications," *Progress Oceanogr.*, vol. 26, no. 3, pp. 263–306, 1991.
[92] P. Chen, C. Jamet, Z. Mao, and D. Pan, "OLE: A novel oceanic Lidar emulator," *IEEE Trans. Geosci. Remote*, pp. 1–15, 2020.
[93] Y. I. Kopilevich and A. G. Surkov, "Mathematical modeling of the input signals of oceanological lidars," *J. Opt. Technol.*, vol. 75, no. 5, pp. 321–326, 2008.
[94] P. Chen *et al.*, "Semi-analytic Monte Carlo radiative transfer model of laser propagation in inhomogeneous sea water within subsurface plankton layer," *Opt. Laser Technol.*, vol. 111, pp. 1–5, 2019.
[95] A. A. Kokhanovsky, "Analytical solutions of multiple light scattering problems: A review," *Meas. Sci. Technol.*, vol. 13, no. 2, pp. 233–240, 2002.
[96] C. Fu *et al.*, "Simulation research on airborne LiDAR bathymetry system," *J. Syst. Simul.*, vol. 27, no. 5, pp. 1038–1043, 2015.

Guoqing Zhou (Senior Member, IEEE) received the Ph.D. degree in photogrammetry and remote sensing from Wuhan University, Wuhan, China, in 1994.

He was a Visiting Scholar with the Department of Computer Science and Technology, Tsinghua University, Beijing, China, and a Post-doctoral Researcher with the Institute of Information Science, Beijing Jiaotong University, Beijing, China. He continued his research as an Alexander von Humboldt Fellow with the Technical University of Berlin, Berlin, Germany, from 1996 to 1998, and was a Post-doctoral Researcher with The Ohio State University, Columbus, OH, USA, from 1998 to 2000. He was an Assistant Professor, an Associate Professor, and a Full Professor with Old Dominion University, Norfolk, VA, USA, in 2000, 2005, and 2010, respectively. He has authored nine books and more than 430 refereed papers.

Chenyang Li was born in Hebei, China, in 1990. He is currently working toward the Ph.D. degree in marine environment science and techology with the School of Marine Science and Technology, Tianjin University, Tianjin, China.

His research interests include airborne LiDAR waveform data processing, the character of blue-green LiDAR transmission through underwater, and the methods and applications of LiDAR bathymetry.

Dianjun Zhang was born in Shandong, China, in 1986. He received the M.S. and Ph.D. degrees in geographical information system from the Institute of Geographic Sciences and Natural Resources Research, Chinese Academy of Sciences, Beijing Forestry University, Beijing, China, in 2011 and 2015, respectively.

His research interests include ocean remote sensing and ship recognition based on deep learning methods.

Dequan Liu received the B.S. degree in electronic science and technology from Northwest Normal University, Lanzhou, China, in 2004, and the M.E. degree in signal and information processing from Xidian University, Xi'an, China, in 2013. He is currently working toward the Ph.D. degree in circuits and systems with the School of Microelectronics, Tianjin University, Tianjin, China.

Xiang Zhou received the M.S. degree in the detection technology and automatic equipment from the Guilin University of Technology, Guilin, China, in 2014.

He is currently with the School of Microelectronics, Tianjin University, Tianjin, China. His research interests include LiDAR imaging.

Jie Zhan was born in Yantai, Shandong, China, in 1997. She received the B.S. degree in geomatics engineering from Shandong University of Science and Technology, Qingdao, China, in 2019. She is currently working toward the M.S. degree in marine techology with the School of Marine Science and Technology, Tianjin University.

Her research interests include ocean color remote sensing and inversion algorithms.